Detoxification, active uptake, and intracellular accumulation of chromium species by a methane-oxidizing bacterium.

ENBAIA, Salaheldeen, ESWAYAH, Abdurrahman, HONDOW, Nicole, GARDINER, Philip <http://orcid.org/0000-0002-2687-0106> and SMITH, Thomas <http://orcid.org/0000-0002-4246-5020>

Detoxification, active uptake, and intracellular accumulation of chromium species by a methane-oxidizing bacterium

Salaheldeen Enbaia [a], Abdurrahman Eswayah [a, b], Nicole Hondow [c], Philip H. E. Gardiner [a], and Thomas J. Smith *[,a].

[a] Biomolecular Sciences Research Centre, Sheffield Hallam University, Howard Street, Sheffield S1 1WB, United Kingdom.

[b] Biotechnology Research Centre, Tripoli, Libya.

[c] School of Chemical and Process Engineering, University of Leeds, Leeds LS2 9JT, United Kingdom.

* Address correspondence to Thomas J. Smith, t.j.smith@shu.ac.uk

Running title: Interaction of chromium with *Methylococcus capsulatus*

Abstract

Despite the wide-ranging proscription of hexavalent chromium, chromium (VI) remains among the major polluting heavy metals worldwide. Aerobic methane-oxidizing bacteria are widespread environmental microorganisms that can perform diverse reactions using methane as the feedstock. The methanotroph *Methylococcus capsulatus* Bath, like many other microorganisms, detoxifies chromium (VI) by reduction to chromium (III). Here, the interaction of chromium species with *M. capsulatus* Bath was examined in detail by using a range of techniques. Cell fractionation and HPLC-inductively coupled plasma-mass spectrometry (HPLC-ICP-MS) indicated that externally provided chromium (VI) underwent reduction, and was then taken up into the cytoplasmic and membranous fractions of the cells. This was confirmed by X-ray photoelectron spectroscopy (XPS) of intact cultures that indicated negligible chromium on the surface of, or outside, the cells. Distribution of chromium and other elements within intact and sectioned cells, as observed via transmission electron microscope (TEM) combined with energy-dispersive X-ray spectroscopy (EDX), and electron energy loss spectroscopy (EELS), was consistent with the cytoplasm/membrane location of the chromium (III), possibly as chromium phosphate. The cells could also take up chromium (III) directly from the medium in a metabolically dependent fashion, and accumulate it within the cells. These results indicate a novel pattern of interaction with chromium species distinct from that observed previously with other microorganisms. They also suggest that *M. capsulatus*, and similar methanotrophs may contribute directly to chromium (VI) reduction, and accumulation in mixed communities of microorganisms that are able to perform methane-driven remediation of chromium (VI).

42 **Importance**

43 *M. capsulatus* Bath is a well characterised aerobic methane-oxidising bacterium that
44 has become a model system for biotechnological development of methanotrophs to
45 perform useful reactions for environmental clean-up, and making valuable chemicals
46 and biological products using methane gas. Interest in such technology has
47 increased recently owing to increasing availability of low-cost methane from fossil,
48 and biological sources. Here, it is demonstrated that the ability of this versatile
49 methanotroph to reduce the toxic contaminating heavy metal chromium (VI) to less
50 toxic chromium (III) form occurs at the same time as accumulation of the chromium
51 (III) within the cells. This is expected to diminish the bioavailability of the chromium,
52 and make it less likely to be re-oxidised to the toxic chromium (VI). Thus *M.*
53 *capsulatus* has the capacity to perform methane-driven remediation of chromium-
54 contaminated water, and other materials, and to accumulate the chromium in the
55 low-toxicity chromium (III) form within the cells.

56 **Introduction**

57

58 Despite world-wide regulation of the use of hexavalent chromium in industry, this
59 highly toxic, and bioavailable form of chromium continues to be a substantial
60 environmental problem. Hence, environmental microorganisms that can detoxify, and
61 sequester chromium species are of biotechnological interest. Despite a fall in
62 commercial use of hexavalent chromium *per se*, various forms of chromium are heavily
63 used in industry, especially in the production of chromium-iron alloys such as stainless
64 steel, and the use of chromium (III) salts in leather manufacture. Mining of chromite,
65 the major chromium-containing ore, also causes substantial environmental release of
66 chromium species. Such anthropogenic contamination contains significant hexavalent
67 chromium which may leach into the aqueous environment (1, 2). Chromium (III), from
68 natural or human sources, may be solubilised by organic acids produced by living
69 systems, and reoxidized in the soil under oxic conditions, particularly in the presence
70 of manganese compounds that can mediate O_2-driven oxidation of chromium (III) to
71 chromium (VI) (3–5). Siderophores, which naturally act as microbial iron-scavenging
72 molecules, can also bind, and solublise chromium (III) (6). In most jurisdictions the
73 maximum contaminant level (MCL) for chromium (VI) in drinking water has not been
74 fixed, though 10 µg litre^{-1}, which was in force in California between 2014, and 2017,
75 has been used as a benchmark of the safe level of chromium (VI) (7). Substantial
76 concentrations of Cr (VI) are found in groundwater, for example up to 1 mg litre^{-1} in
77 certain areas of California (7), and up to 34 µg litre^{-1} in drinking water wells in the
78 Piedmont area of North Carolina (8). The particulate fraction of the exhaust from
79 biodiesel combustion may contain up to 2 mg/g of chromium (9). Worldwide, waste

80 materials, and contaminated sites requiring remediation have reported chromium (VI)
81 concentrations up to tens of parts per million (10, 11).

82 Many bacteria can bioremediate chromium (VI) via reduction to the less harmful
83 trivalent form (12). The metabolic diversity of prokaryotes provides a wide range of
84 natural, and artificial electron donors for chromium (VI) reduction (12, 13). Among
85 these, methane is particularly attractive because it is available in large quantities from
86 fossil sources, and biogas. It has aroused greater interest in recent years due to falling
87 methane prices (14). Aerobic methanotrophs, a diverse group of environmental
88 bacteria that are able to use methane as their carbon and energy source, are
89 significant as a global methane sink. Methanotrophs and their enzymes have been
90 explored for a range of biotechnologically valuable methane-driven processes
91 including bioremediation, production of single-cell protein and as catalysts for
92 oxygenation of unfunctionalized carbon atoms in organic molecules (15–19).

93 The γ-proteobacterial methanotroph *Methylococcus capsulatus* Bath is able to reduce
94 chromium (VI) to chromium (III) over a wide range of concentrations (tested across 1.4
95 to 1,000 mg litre^{-1}) (20). Methane-driven chromium (VI) reduction has also been
96 achieved in a methane-fed polymicrobial biofilm reactor system (21), where some of
97 the reduction of Cr (VI) is attributed to non-methanotrophs scavenging nutrients
98 (multicarbon compounds, and more generally accessible C1 substrates such as
99 methanol) produced by the methanotrophs.

100 Methanotrophs are known to bind, and transform a range of toxic metals, and
101 metalloids in addition to chromium. The α-proteobacterial methanotrophs such as
102 *Methylosinus trichosporium* OB3b produce a range of structurally related copper-

103 scavenging molecules termed methanobactins (22). Methanobactin-bound copper is
104 in the +1 oxidation state; binding of Cu (II) to methanobactin results in its reduction to
105 Cu (I) (23), possibly by electrons derived from water (22). Methanobactin is able to
106 bind a wide range of cations; a subset of these, including Hg (II), Au (III), undergo
107 reduction upon binding, in a similar manner to copper, to give metallic mercury and
108 metallic gold nanoparticles, respectively (24–27). Methanobactin binds methyl
109 mercury ($MeHg^+$); in *M. trichosporium* methanobactin is necessary for detoxification of
110 $MeHg^+$ as well as promoting *in-vivo* methylation of Hg (II) (24, 27, 28). The γ-
111 proteobacterial methanotroph *M. capsulatus* Bath reduces Hg^{2+} ions to metallic
112 mercury (29) and takes up but does not detoxify $MeHg^+$. Methanotrophs respond to
113 lanthanide elements that are required for activity of a key metabolic methanol
114 dehydrogenase (25, 30, 31). They also convert selenite (SeO_3^{2-}) to selenium-
115 containing nanoparticles and volatile methylated selenium species (32, 33).

116 Previous work on remediation of Cr (VI) by *M. capsulatus* Bath showed that chromium
117 (III) accumulated in the particulate fraction of the culture, and (based on extended X-
118 ray absorption spectroscopy fine structure [EXAFS] results) was likely coordinated by
119 oxygen, and phosphorous (20). Previously, electron microscopy techniques coupled
120 to spectroscopic analysis have been used with other systems to characterise the
121 distribution, and speciation of chromium associated with bacteria at the cellular or
122 subcellular level (21, 34–37). Here, we have used a range of cell fractionation,
123 analytical, electron microscope, and spectroscopic techniques to obtain spatially
124 resolved information about the interaction of chromium species with *M. capsulatus*, to
125 determine how its specific properties might be exploited for bioremediation, and to gain
126 insights into the role such methanotrophs may play in the environmental chromium
127 cycle.

128

129 **Results**

130

131 **Effect of concentration on chromium (VI) removal**

132 HPLC-ICP-MS is a well-established technique for quantifying and determining the
133 speciation of heavy metals and other elements that has been previously used to
134 characterise reduction of chromium (VI) at a bulk culture level (for example (38)). In
135 order to characterise range of chromium (VI) concentrations over which *M. capsulatus*
136 could remediate all or most of the added chromium (VI), various concentrations of
137 chromium (VI) were added to cultures of *M. capsulatus* Bath (OD_{600} of 0.7- 0.9), and
138 then the cultures were incubated at 45°C in the presence of methane and air.
139 Chromium species in the culture supernatant were quantified by using HPLC-ICP-MS
140 (Fig. 1). *M. capsulatus* Bath achieved complete removal of detectable chromium (VI)
141 at initial concentrations up to 5 mg litre^{-1}, and was able to substantially decrease the
142 chromium (VI) of the culture supernatant from initial concentrations ≤40 mg litre^{-1}. No
143 other detectable chromium species appeared in the culture supernatant. A
144 concentration of chromium (VI) of 20 mg litre^{-1} was chosen for further experiments
145 since this gave the largest amount of chromium (VI) removed within 144 h.

146 **Reduction and accumulation of chromium species within cellular fractions**

147 In order to gain more information about the possible location of chromium species
148 within the culture, cultures were incubated with an initial concentration of chromium
149 (VI) of 20 mg litre^{-1} and samples were taken over a time course of 144 h. Cells within
150 each sample were then broken and separated into cell walls and a combined fraction

151 of membranes+cytoplasm, as detailed in the Materials and Methods, before
152 quantifying the chromium species via HPLC-ICP-MS (Fig. 2).

153 Over a period of 144 h, the concentration of chromium (VI) in the culture supernatant
154 declined, while there was a corresponding increase in the concentration of chromium
155 (III) in the cytoplasm+membranes fraction. No other chromium species were detected
156 in significant concentrations in any of the samples. The constant total chromium (the
157 sum of the chromium detected in all fractions) (Fig. 2) indicates that the appearance
158 of chromium (III) in the cytoplasm+membranes fraction accounted, within experimental
159 error, for the decrease in chromium (VI) in the culture supernatant. Hence cells of *M.*
160 *capsulatus* Bath were able not only to reduce chromium (VI) to chromium (III) but
161 appeared able to accumulate all the chromium (III) within the biomass.

162 To gain additional information about the location of chromium species within the cells,
163 cultures were exposed to chromium (VI) (20 mg litre^{-1}), and cells were fractionated to
164 produce separate membrane and cytoplasm fractions. The results showed that the
165 distribution of chromium (III) between the two fractions was approximately two thirds
166 in the cell membrane fraction and one third in the cytoplasm fraction (Fig. 3).

167

168 **Uptake of Cr (III)**

169 The fact that all of the cell-associated chromium was in the +3 oxidation state, even
170 though the cells had been exposed to chromium in the hexavalent form, raised the
171 question of whether reduction and uptake of chromium were necessarily linked, or
172 whether cells could take up trivalent chromium directly. When exposed in exactly the
173 same way to 20 mg litre^{-1} of chromium (III) in the presence of methane and air, the *M.*

174 *capsulatus* cells took up the chromium (III) completely into the cytoplasm+membranes
175 fraction within 1 h (Fig. 4A), much more quickly than >144 h taken for reduction and
176 accumulation of the same amount of chromium (VI). Previous work has shown that
177 the reduction of chromium (VI) to chromium (III) by *M. capsulatus* Bath is an active
178 process requiring the presence of the carbon and energy source methane (20). In
179 order to investigate whether the uptake of chromium (III) was also an active process,
180 cultures were exposed to 20 mg litre^{-1} of chromium (III) aerobically though in the
181 absence of methane. If the cells were grown to OD_{600} 0.7- 0.9 in the presence of
182 methane and then methane was removed and chromium (III) added immediately, all
183 the chromium (III) was taken up by the cells within 1 h (Fig. 4B). If, however, the cells
184 were starved of methane overnight (16 h) before addition of the chromium (III), only
185 25 % of the chromium (III) was taken up (Fig. 4C). Addition of the metabolic inhibitor
186 sodium azide to 0.05% w/v (Fig. 4D) abolished approximately half of the uptake of
187 chromium (III) within a 1 h period. When the cells were both starved of methane
188 overnight and sodium azide was added at the same time as the chromium (III), uptake
189 of chromium (III) was completely abolished (Fig. 4E). Heat-killing (autoclaving) of the
190 cells also completely abolished chromium (III) uptake (Fig. 4F). These results indicate
191 that uptake of chromium (III) is an active process, but that when methane is removed
192 from a growing culture, it has sufficient reserves of energy to take up a substantial
193 amount of chromium (III).

194 **Spatially resolved spectroscopic characterisation of the cells**

195 EELS coupled with TEM of whole *M. capsulatus* Bath cells exposed to 20 mg litre^{-1} of
196 chromium (VI) for 96 h or 144 h confirmed, via comparison with spectra of chromium
197 standards, that the cell-associated chromium was in the +3 oxidation state (Fig. 5).
198 Cells exposed to 20 mg litre^{-1} of chromium (VI) for 144 h were also prepared as thin
199 sections to see how chromium and other elements were distributed within the cells.
200 HAADF-STEM-EDX showed the presence of chromium in the chromium-treated cells,
201 and its absence from the chromium-untreated control (Fig. 6). The spatial distribution
202 of chromium (Fig. 6C) indicated that the chromium was largely cell-associated and
203 distributed throughout the cell. This is consistent with the approximate 40:60
204 distribution of the chromium between the cytoplasm and membrane fractions, when it
205 is born in mind that *M. capsultus* Bath under pMMO expressing conditions of these
206 experiments is expected to have intracellular as well as peripheral membranes (19).

207 The spatial distribution of chromium, and a number of other elements (carbon,
208 phosphorous and oxygen) was also determined within whole *M. capsulatus* cells via
209 EDX (Figs. S1-S4). These results indicated that there was inhomogeneity in the
210 distribution of all four elements, which appeared to correlate with structural features
211 of the cells visible in the electron micrographs. Since these features showed
212 elevated concentrations of chromium, phosphorous and oxygen and decreased
213 concentrations of carbon, they are consistent with the deposition of chromium
214 phosphate (containing Cr, O and P) associated with the cells. This is also consistent
215 with the phosphorous and oxygen ligation of *M. capsulatus* cell-associated chromium
216 (III) inferred from EXAFS data (20). The EDX analysis also indicated an increase in
217 calcium associated with the cells that had been exposed to chromium (Figs. S1-S4).

218 Surface analysis of samples of *M. capsulatus* cells treated with 20 mg litre^{-1} of
219 chromium (VI) was performed, in comparison with chromium-untreated samples, by
220 using XPS (Figs. S5 and S6; Tables S1 and S2). Whilst the depth of penetration of
221 XPS into the sample is small (several nm), the areas of data acquisition were 400
222 μm in diameter. This is large compared to the cells (approximate diameter 1 μm)
223 and so these data show the properties of the surface of the whole sample rather than
224 individual cells, and subcellular structures seen by other techniques.

225 The carbon and oxygen X-ray photoelectron spectra of chromium (VI)-treated and
226 chromium (VI)-untreated cells show features that are consistent with the presence of
227 peptides, carbohydrates, lipids, and phosphate groups that are likely to be associated
228 with the surface of the cells (Tables S1 and S2). The signals at binding energies of
229 400.1 eV (chromium (VI)-treated sample), and 399.8 eV (chromium (VI)-untreated
230 sample) were attributed to N 1s, which is widely found in amino acids, and amino
231 sugars (amino sugars are found in cell wall peptidoglycan, and amino acids are
232 constituents of both peptidoglycan and proteins) (Figs. S5 and S6). No substantial
233 differences in the spectra of carbon, oxygen or nitrogen were observed between the
234 chromium (VI)-treated, and -untreated cells (Figs. S5 and S6; Tables S1 and S2).

235 Most notably, the small peak at binding energy 577.8 eV in the chromium (VI)-treated
236 sample (Fig. S5 parts A and E), which may be due to emission of photoelectrons from
237 the 2p orbitals of chromium, was not substantially above the noise in the baseline of
238 the spectrum. This indicates presence of very little chromium on the surface of the
239 cells, which is consistent with the results from analysis of the cell fractions that suggest
240 that chromium is within the cells, associated with the membranes and cytoplasm.

241

242 **Discussion**

243 The results reported here indicate the capacity of *M. capsulatus* Bath to reduce
244 chromium (VI) at concentrations up to several mg litre^{-1} or mg g^{-1}, which are relevant
245 to current contaminated groundwater and solid waste problems (7, 9–11). *M.*
246 *capsulatus* Bath can, for example, take the concentration of hexavalent chromium
247 from 3 mg litre^{-1} to below the level of detection of HPLC-ICP-MS ($\leq$ 0.005 mg litre^{-1} in
248 these experiments) within 48 h (Fig. 1). The nearly straight plots of C/C_0 vs. time
249 (Fig. 1) at $\leq$10 mg litre^{-1} initial chromium concentration suggest near zero order
250 kinetics at these low chromium concentrations. The rate of chromium (VI) removal
251 during the first 48 h of incubation (Fig. S7) shows a dependence of chromium (VI)
252 removal on the initial concentration, with a maximum at 20 mg litre^{-1} and a clear
253 decline as the system becomes inhibited at higher concentrations of chromium (VI).
254 In these experiments total removal of detectable chromium (VI) was not achieved
255 within 144 h from an initial concentration of 10 mg litre^{-1} or above. Although no
256 significant removal of chromium (VI) was observed from an initial chromium
257 concentration of 50 mg litre^{-1}, reduction of a small proportion of added chromium (VI)
258 by *M. capulatus* must be possible at higher concentrations since the cells from a
259 culture exposed to 1,000 mg litre^{-1} of chromium (VI) contained chromium solely in
260 the +3 oxidation state, although the amount of chromium (VI) reduced within the
261 culture was not measured (20).

262 Previously, BLAST sequence similarity searches of the *M. capsulatus* Bath genome
263 with representatives of three classes of chromium (VI) reductases and a chromate
264 efflux pump were performed, to identify proteins possibly involved in reduction of
265 chromium (VI) (20). Since the genome of *M. trichosporium* OB3b (39), which does

266 not reduce chromium (VI) (20), is now available this analysis was repeated with both
267 genomes in parallel (Table S3). The number of potential chromate reductases
268 identified in the genome of each organism is the same. Also, neither has a
269 homologue of the chromate efflux pump. The ChrA chromate reductase of
270 *Pseudomonas putida* (40) has a homologue in *M. trichosporium* OB3b but not in *M.*
271 *capsulatus* Bath. The Fre chromate reductase of *Escherichia coli* (41) has only two
272 homologues in *M. trichosporium* OB3b but three in *M. capsulatus* Bath. Amongst
273 these, *M. capsulatus* alone has the gene encoding a putative subunit F of an Na^+-
274 translocating NADH-quinone reductase, which is part of a six-gene cluster encoding
275 a possible transmembrane complex that that transfers electrons between NADH and
276 quinones (42) that is missing from *M. trichosporium* OB3b. One possibility is that
277 chromium (VI) reduction in *M. capsulatus* Bath is an adventitious activity of this
278 complex, although it is also possible that other factors (such as the access of
279 chromium [VI] to the reductase due to permeability properties) are the reason that *M.*
280 *trichosporium* OB3b cells do not reduce chromium. The complexity of the reaction
281 kinetics is consistent with a system in which the rate is influenced by multiple factors,
282 such as enzyme activities, permeability and toxicity.

283 Here, as in other studies HAADF-STEM-EDX has been used to study the distribution
284 of metals in bacterial cells (33, 43, 44). The formation of cell-associated structures
285 composed of precipitated metal ions has been observed previously, such as
286 chromium-containing particles on the surface of a chromium (VI)-
287 reducing *Pseudomaonas synxantha* (45), and extracellular fibres and stalks of Fe
288 (III) oxides by *Gallionella* (46). Chromium (VI)-exposure of *S. oneidensis* (35) and
289 *Desulfovibrio vulgaris* (36) also results in deposition of chromium (III) in the form of
290 precipitate on the surface of the cells, although intracellular chromium (II) has been

291 observed under strictly anaerobic conditions in *S. oneidensis* and may be an
292 intermediate in the conversion of chromium (VI) under conditions where the
293 extracellular precipitated chromium (III) is produced by this organism (43). The
294 cellular breakage and fractionation technique used here with *M. capsulatus* Bath
295 showed the presence of all detectable chromium, after cell breakage, as chromium
296 (III) within soluble cell-associated material and in association with membranes (or
297 other small cell-derived particulate material with similar sedimentation properties).
298 Whilst the possibility of redistribution of chromium (III) after breakage of the cells
299 cannot be excluded, the absence of extracellular precipitated chromium-containing
300 material from TEM images, together with the shielding of chromium from XPS, give
301 strong independent evidence of the intracellular location of the chromium (III)
302 product. This intracellular chromium (III), which may be in the form of chromium (III)
303 phosphate or as chromium associated with organic phosphate groups, is visible to
304 EDX and EELS in whole cells as these are transmission techniques (results
305 generated throughout the thickness of the sample).

306 *M. capsulatus* Bath was originally isolated from the Roman baths in Bath, UK, which
307 are fed by water from a geothermal spring that is consistently low in toxic heavy
308 metals, including chromium (<0.5 μg litre^{-1}) (47). A strain of *Methylomonas koyamae*
309 capable of removing chromium (VI) has also been isolated from river sediment with
310 substantial heavy metal pollution (including chromium at up to 25 mg kg^{-1}) (48).
311 Hence, chromium (VI)-removing methanotrophs can be found in environments with
312 greatly differing heavy metal contamination.

313 A number of studies have reported methane-driven chromium (VI) reduction by
314 mixed communities of microorganisms (21, 49–51). These studies have attributed

315 chromium (VI) reduction in such communities to the activities of non-methanotrophs.
316 The fact that a pure methanotroph strain is able to reduce chromium (VI) (20)
317 indicates that methanotrophs may contribute to methane-driven chromium (VI)
318 reduction in polymicrobial communities, including those which may occur naturally in
319 the environment. Studies of methane-driven reduction of chromium (VI) by mixed
320 communities of microorganisms have shown that the bulk of the chromium in such
321 polymicrobial systems is in the form of extracellular precipitate that is visible to XPS
322 (21), in contrast to the intracellular location of the chromium (III) in pure cultures of
323 *M. capsulatus* Bath.

324 Intracellular sequestration of chromium (III) by *M. capsulatus* Bath may help to
325 reduce its bioavailiabilty to other organisms and, since immobilisation of chromium
326 (III) has been linked to preventing its environmental reoxidation (3), likely make it
327 less susceptible to reoxidation to chromium (VI). It is also possible that, under
328 environmental conditions on a sufficiently long timescale, the cell-associated
329 chromium (III) may be released into the environment.

330 Whilst it is generally accepted that chromium (III) is of lower toxicity than chromium
331 (VI), previous studies have indicated detectable genotoxicity of chromium (III) to
332 *Escherichia coli* (52), toxicity through generation of reactive oxygen species in Gram-
333 positive and Gram-negative bacteria (53) and causing harmful morphological
334 changes in *Shewanella oneidensis* (54). Hence, it is likely that the cells are
335 substantially damaged by their uptake of chromium (III). They evidently maintain
336 sufficient metabolism to allow the observed reduction and accumulation of chromium
337 species observed, though it may be accumulation of the chromium (III) within the

338 cells that causes decline in chromium (VI) removal as the externally applied
339 chromium (VI) concentration is increased.

340 Previously, removal of chromium (III) by microorganisms has been largely attributed
341 to adsorption to biomass, for example, biofilms of *Bacillus subitilis* were found more
342 effective in immobilising chromium (III) produced from reduction of chromium (VI)
343 than planktonic cells, possibly owing to adsorption to extrapolymeric substances
344 within the biofilm (55). The results with *M. capsulatus* suggest a rather different
345 pattern where uptake of external chromium (III) into the interior of the cell (cytoplasm
346 and membranes) is an active process. Since most studies of chromium (VI)
347 bioremediation have not investigated what happens if chromium (III) is added, it may
348 be that active uptake of chromium (III) is found in other microorganisms also. The
349 presence of chromium (III) to a substantial extent in soluble form in the cytoplasm
350 fraction of *M. capsulatus* is consistent with observations that organic acids, amino
351 acids and other small biomolecules can maintain chromium (III) in soluble form in the
352 presence of macromolecular biomass (56).

353 In order to establish the pathway of electrons between methane and chromium (VI),
354 it will be necessary to identify the enzymes involved. Additionally, the effects of the
355 availability of copper and lanthanides (which control the expression of different forms
356 of methane monooxygenase, respectively) (30, 57–59), may offer a means of
357 studying the pathway of electrons into chromium (VI) reduction.

358 Work in recent years has highlighted the key environmental role played in the
359 environmental cycling of metals by aerobic methanotrophs (30), which show a much
360 greater diversity than was previously realised (16). This study has shown that one

member of this important group of organisms shows a novel pattern of interaction with chromium species that may make it suitable for applications in bioremediation of chromium species and open the possibility for a role for methanotrophs in transformation and bioavailablity of chromium species in the environment.

366 **Materials and methods**

367 **Bacterial strains and growth conditions**

368 The methanotrophic bacterium *M. capsulatus* Bath was grown aerobically at 45 °C in
369 sterile nitrate mineral salts (NMS) medium with shaking (180 rpm), or NMS agar plates
370 inside airtight jars, as described previously (60). Methanotrophs such as *M.*
371 *capsulatus* Bath have "copper switch" that controls the expression of the membrane-
372 associated copper-dependent particulate methane monooxygenase (pMMO) vs. the
373 cytoplasmic iron-dependent soluble methane monooxygenase (sMMO) on the basis
374 of the copper-to-biomass ratio of the culture (57, 61). In our hands, flask cultures
375 grown in the copper concentration of 0.4 μM the NMS used here do not attain the cell
376 density needed to express sMMO and so the experiments described were performed
377 under pMMO-expressing conditions. Chromium (VI) bioremediation experiments were
378 performed in 50 ml liquid cultures in 250 ml conical Quickfit flasks capped with Suba-
379 Seals (Sigma-Aldrich). Plates were incubated in a 1:4 v/v methane:air mixture. To add
380 methane to flasks, 50 ml of headspace gas was removed, after which 60 ml of methane
381 was added (60). Liquid cultures (50 ml) were grown to late logarithmic phase (OD_{600}
382 of 0.6-0.9), which typically took 40-48 h. Chromium species were added from filter
383 sterilised stock solutions containing 1,000 mg litre^{-1} of Cr (K_2CrO_4 for Cr (VI), and
384 $Cr(NO_3)_3$ for Cr (III)) to the concentrations stated for each experiment.

385 **Quantitation, and characterization of chromium species**

386 Separation and quantification of aqueous chromium (VI) and chromium (III) was
387 achieved via ion exchange HPLC coupled to ICP-MS, as follows. An aliquot of the
388 sample (20 µl) was injected with a PerkinElmer LC Flexar autosampler into a

389 PerkinElmer Flexar HPLC pump attached to a Hamilton PRP-X100 column, 4.6 × 250
390 mm, and coupled to a PerkinElmer ICP-MS NexION 350X. The column flow rate was
391 1.2 ml min^{-1}; the mobile phase was 0.5 mmol $litre^{-1}$ ethylenediamine-tetraacetic acid
392 disodium salt (Na_2-EDTA) containing nitric acid (70 % w/w, 0.875 ml per litre of
393 solution); aqueous ammonia was added to adjust the pH to 7. The limit of detection
394 was 0.01 mg $litre^{-1}$ for chromium (III) and 0.005 mg $litre^{-1}$ for chromium (VI).

395 **Fractionation of cultures, and cells**

396 Aliquots (5 ml) of cultures exposed to chromium (VI) or chromium (III) species as
397 detailed above were collected at intervals, and centrifuged (11,000 × *g*; 10 min; room
398 temperature), to remove cells and other debris. The remaining culture supernatant
399 was analysed via HPLC-ICP-MS as detailed above.

400 Cells were fractionated via a modification of a published method (62), as follows. The
401 whole process was performed at 0-4°C, to minimise sample degradation. Harvested
402 cell pellets from 5 ml samples of culture were washed with 5 ml of 25 mM MOPS (pH
403 7), centrifuged (11,000 × *g*; 10 min), and resuspended in 5 ml of the same buffer. The
404 suspension was passed twice through a French pressure cell (8.2 MPa) in order to
405 break the cell walls. The suspension of broken cells was centrifuged (3,000 × *g*, twice
406 for 2 min each) to remove unbroken cells before being centrifuged (27,000 × *g*, 20
407 min) to sediment cell wall fragments and any other large broken cell fragments. The
408 pellet was washed twice by resuspension in 25 mM MOPS (pH 7) and then
409 resuspended in the same buffer; the resulting fraction was used as the cell wall fraction.
410 The supernatant from the first centrifugation after cell breakage, which contained the
411 cytoplasm and membrane fragments, was centrifuged again (27,000 × *g*, 20 min) to

412 remove remaining large particulate material. The resulting supernatant was used as
413 the cytoplasm+membranes fraction. When cytoplasm and membranes were analysed
414 separately, this fraction was further separated via ultracentrifugation at 105,000 × *g* for
415 60 min. The pellet was washed in 25 mM MOPS (pH 7), ultracentrifuged again under
416 the same conditions, resuspended in the same buffer to give the cell membrane
417 fraction. The supernatant from the first ultracentrifugation was centrifuged again under
418 the same conditions to remove remaining membranous material, to give the the
419 cytoplasm fraction.

420 **Imaging, and surface analysis**

421 For electron microscopy, cells from samples (5 ml) of chromium (VI)-exposed cultures,
422 and control cultures without chromium were pelleted by centrifugation (11,000 × *g*; 10
423 min; room temperature), and washed under the same conditions with 0.1 M sodium
424 phosphate buffer (pH 7.4). The specimens were then fixed in 3% glutaraldehyde in the
425 same buffer overnight at room temperature, and washed again under the same
426 conditions in the same buffer. Secondary fixation was carried out in 1% w/v aqueous
427 osmium tetroxide for 1 h at room temperature followed by the same washing procedure.
428 Fixed cells were dehydrated through a graded series of ethanol dehydration steps (75,
429 95 and 100% v/v), and then placed in a 50/50 (v/v) mixture of ethanol and
430 hexamethyldisilazane followed by 100% hexamethyldisilazane. The specimens were
431 then allowed to air dry overnight. A small portion of the fixed sample was crushed, and
432 dispersed in methanol, with a drop placed on a holey carbon-coated copper grid (Agar
433 Scientific). Transmission electron microscopy (TEM) was conducted on an FEI Titan^3
434 Themis G2 operating at 300 kV fitted with 4 EDX silicon drift detectors, a Gatan One-
435 View CCD, and a Gatan GIF quantum ER 965 imaging filter for electron energy loss

436 spectroscopy (EELS). Energy-dispersive X-ray (EDX) spectroscopy, and mapping
437 were undertaken using Bruker Esprit v1.9 software, and a high-angle annular dark-
438 field (HAADF) scanning TEM (STEM) detector.

439 For thin section analysis, after the ethanol dehydration steps, the cells were embedded
440 in EM bed 812 epoxy resin, and cut into thin sections (90 nm) using a diamond knife
441 on a Reichert Ultracut S ultramicrotome. The sections were supported on copper grids,
442 and coated with carbon. The samples were examined in an FEI Tecnai F20 field
443 emission gun (FEG) transmission electron microscope operating at 200 kV, and fitted
444 with a Gatan Orius SC600A charge-coupled-device (CCD) camera, an Oxford
445 Instruments XMax SDD energy-dispersive X-ray (EDX) detector, and a HAADF-STEM
446 detector.

447 XPS measurements were made on a KRATOS SUPRA Photoelectron Spectrometer
448 at 10 kV and 20 mA using a monochromatic Al K (alpha) X-ray source (1486.6 eV).
449 The take-off angle was fixed at 90 degrees. On each sample the data were collected
450 from three randomly selected locations, and the area corresponding to each
451 acquisition was 400 micrometres in diameter. Each analysis consisted of a wide
452 survey scan (pass energy 160 eV, 1.0 eV step size), and high-resolution scan (pass
453 energy 20 eV, 0.1eV step size) for component speciation. The binding energies of the
454 peaks were determined using the C1s peak at 284.5 eV. The software Casa XPS
455 2.3.17 was used to fit the XPS spectra peaks. No constraint was applied to the initial
456 binding energy values, and the full width at half maximum (fwhm) was maintained
457 constant for the carbon contributions in a particular spectrum.

458 **Bioinformatics**

459 BLAST searches of the proteins encoded by the *M. capsulatus* Bath and *M.*
460 *trichosporium* OB3b genomes were conducted via the IMG platform (63).

Disclosures

The authors declare no competing financial interests.

Acknowledgements

SE gratefully acknowledges financial support from the Libyan Government in the form of a PhD scholarship. We thank Michael Cox (Sheffield Hallam University) for assistance with HPLC-ICP-MS measurements. We thank Chris Hill (University of Sheffield) for sectioning samples for TEM.

References

1. Beukes JP, du Preez SP, van Zyl PG, Paktunc D, Fabritius T, Päätalo M, Cramer M. 2017. Review of Cr(VI) environmental practices in the chromite mining and smelting industry – Relevance to development of the Ring of Fire, Canada. J Clean Prod 165:874–889.

2. Coetzee JJ, Bansal N, Chirwa EMN. 2020. Chromium in environment, its toxic effect from chromite-mining and ferrochrome industries, and its possible bioremediation. Expo Heal 12:51–62.

3. Varadharajan C, Beller HR, Bill M, Brodie EL, Conrad ME, Han R, Irwin C, Larsen JT, Lim HC, Molins S, Steefel CI, Van Hise A, Yang L, Nico PS. 2017. Reoxidation of chromium(III) products formed under different biogeochemical regimes. Environ Sci Technol 51:4918–4927.

482 4. Hausladen DM, Fendorf S. 2017. Hexavalent chromium generation within
483 naturally structured soils and sediments. Environ Sci Technol 51:2058–2067.

484 5. Wadhawan AR, Stone AT, Bouwer EJ. 2013. Biogeochemical controls on
485 hexavalent chromium formation in estuarine sediments. Environ Sci Technol
486 47:8220–8228.

487 6. Duckworth OW, Akafia MM, Andrews MY, Bargar JR. 2014. Siderophore-
488 promoted dissolution of chromium from hydroxide minerals. Environ Sci
489 Process Impacts 16:1348–1359.

490 7. Hausladen DM, Alexander-Ozinskas A, McClain C, Fendorf S. 2018.
491 Hexavalent Chromium Sources and Distribution in California Groundwater.
492 Environ Sci Technol 52:8242–8251.

493 8. Vengosh A, Coyte R, Karr J, Harkness JS, Kondash AJ, Ruhl LS, Merola RB,
494 Dywer GS. 2016. Origin of hexavalent chromium in drinking water wells from
495 the Piedmont aquifers of North Carolina. Environ Sci Technol Lett 3:409–414.

496 9. Agarwal AK, Singh AP, Gupta T, Rashmi A. 2018. Mutagenicity and
497 Cytotoxicity of particulate matter emitted from biodiesel-fueled engines.
498 Environ Sci Technol 52:14496–14507.

499 10. Dhal B, Thatoi HN, Das NN, Pandey BD. 2013. Chemical and microbial
500 remediation of hexavalent chromium from contaminated soil and
501 mining/metallurgical solid waste: A review. J Hazard Mater 250–251:272–291.

502 11. Jobby R, Jha P, Yadav AK, Desai N. 2018. Biosorption and biotransformation
503 of hexavalent chromium [Cr(VI)]: A comprehensive review. Chemosphere
504 207:255–266.

505 12. Cervantes C, Campos-García J, Devars S, Gutiérrez-Corona F, Loza-Tavera
506 H, Torres-Guzmán JC, Moreno-Sánchez R. 2001. Interactions of chromium
507 with microorganisms and plants. FEMS Microbiol Rev 25:335–47.

508 13. Zhang HK, Lu H, Wang J, Zhou JT, Sui M. 2014. Cr(VI) reduction and Cr(III)
509 immobilization by acinetobacter sp. HK-1 with the assistance of a novel
510 quinone/graphene oxide composite. Environ Sci Technol 48:12876–12885.

511 14. Risso C, Choudhary S, Johannessen A, Silverman J. 2018. Methanotrophy
512 goes commercial: challenges, opportunities, and brief history, p. 293–298. *In*
513 Kalyuzhnaya, MG, Xing, X-H (eds.), Methane Biocatalysis: Paving the Way to
514 Sustainability. Springer International Publishing, Cham.

515 15. Jiang H, Chen Y, Jiang P, Zhang C, Smith TJ, Murrell JC, Xing X-H. 2010.
516 Methanotrophs: Multifunctional bacteria with promising applications in
517 environmental bioengineering. Biochem Eng J 49:277–288.

518 16. Smith TJ, Murrell JC. 2008. Methanotrophy/methane oxidation, p. 293–298. *In*
519 Encyclopedia of Industrial Microbiology. Wiley.

520 17. Strong PJ, Kalyuzhnaya M, Silverman J, Clarke WP. 2016. A methanotroph-
521 based biorefinery: Potential scenarios for generating multiple products from a
522 single fermentation. Bioresour Technol 215:314–323.

523 18. Kwon M, Ho A, Yoon S. 2019. Novel approaches and reasons to isolate
524 methanotrophic bacteria with biotechnological potentials: recent achievements
525 and perspectives. Appl Microbiol Biotechnol 103:1–8

526 19. Hanson RS, Hanson TE. 1996. Methanotrophic bacteria. Microbiol Rev
527 60:439–471.

528 20. Al Hasin A, Gurman SJ, Murphy LM, Perry A, Smith TJ, Gardiner PHE. 2010.
529 Remediation of chromium(VI) by a methane-oxidizing bacterium. Environ Sci
530 Technol 44:400–405.

531 21. Lai C-Y, Zhong L, Zhang Y, Chen J-X, Wen L-L, Shi L-D, Sun Y-P, Ma F,
532 Rittmann BE, Zhou C, Tang Y, Zheng P, Zhao H-P. 2016. Bioreduction of
533 chromate in a methane-based membrane biofilm reactor. Environ Sci Technol
534 50:5832–5839.

535 22. Semrau JD, Dispirito AA, Obulisamy PK, Kang-Yun CS. 2020. Methanobactin
536 from methanotrophs: Genetics, structure, function and potential applications.
537 FEMS Microbiol Lett 367:1–13.

538 23. El Ghazouani A, Baslé A, Firbank SJ, Knapp CW, Gray J, Graham DW,
539 Dennison C. 2011. Copper-binding properties and structures of
540 methanobactins from *Methylosinus trichosporium* OB3b. Inorg Chem 50:1378–
541 1391.

542 24. Vorobev A, Jagadevan S, Baral BS, Dispirito AA, Freemeier BC, Bergman BH,
543 Bandow NL, Semrau JD. 2013. Detoxification of mercury by methanobactin
544 from *Methylosinus trichosporium* OB3b. Appl Environ Microbiol 79:5918–5926.

545 25. Choi DW, Do YS, Zea CJ, McEllistrem MT, Lee SW, Semrau JD, Pohl NL,
546 Kisting CJ, Scardino LL, Hartsel SC, Boyd ES, Geesey GG, Riedel TP, Shafe
547 PH, Kranski KA, Tritsch JR, Antholine WE, DiSpirito AA. 2006. Spectral and
548 thermodynamic properties of Ag(I), Au(III), Cd(II), Co(II), Fe(III), Hg(II), Mn(II),
549 Ni(II), Pb(II), U(IV), and Zn(II) binding by methanobactin from *Methylosinus*
550 *trichosporium* OB3b. J Inorg Biochem 100:2150–2161.

551 26. McCabe JW, Vangala R, Angel LA. 2017. Binding selectivity of methanobactin
552 from *Methylosinus trichosporium* OB3b for copper(I), silver(I), zinc(II),
553 nickel(II), cobalt(II), manganese(II), lead(II), and iron(II). J Am Soc Mass
554 Spectrom 28:2588–2601.

555 27. Baral BS, Bandow NL, Vorobev A, Freemeier BC, Bergman BH, Herdendorf
556 TJ, Fuentes N, Ellias L, Turpin E, Semrau JD, Dispirito AA. 2014. Mercury
557 binding by methanobactin from *Methylocystis* strain SB2. J Inorg Biochem
558 141:161–169.

559 28. Yin X, Wang L, Zhang L, Chen H, Liang X, Lu X, DiSpirito AA, Semrau JD, Gu
560 B. 2020. Synergistic effects of a chalkophore, methanobactin, on microbial
561 methylation of mercury. Appl Environ Microbiol 86.

562 29. Boden R, Murrell JC. 2011. Response to mercury (II) ions in *Methylococcus*
563 *capsulatus* (Bath). FEMS Microbiol Lett 324:106–110.

564 30. Semrau JD, DiSpirito AA, Gu W, Yoon S. 2018. Metals and methanotrophy.
565 Appl Environ Microbiol 84:7–14.

566 31. Dassama LMK, Kenney GE, Rosenzweig AC. 2017. Methanobactins: from
567 genome to function. Metallomics 9:7–20.

568 32. Eswayah AS, Smith TJ, Scheinost AC, Hondow N, Gardiner PHE. 2017.
569 Microbial transformations of selenite by methane-oxidizing bacteria. Appl
570 Microbiol Biotechnol 101:6713–6724.

571 33. Eswayah AS, Hondow N, Scheinost AC, Merroun M, Romero-González M,
572 Smith TJ, Gardiner PHE. 2019. Methyl selenol as a precursor in selenite
573 reduction to Se/S species by methane-oxidizing bacteria. Appl Environ

574 Microbiol 85:AEM.01379-19.

575 34. Wang Y, Sevinc PC, Belchik SM, Fredrickson J, Shi L, Lu HP. 2013. Single-
576 cell imaging and spectroscopic analyses of Cr(VI) reduction on the surface of
577 bacterial cells. Langmuir 29:950–956.

578 35. Neal AL, Lowe K, Daulton TL, Jones-Meehan J, Little BJ. 2002. Oxidation
579 state of chromium associated with cell surfaces of *Shewanella oneidensis*
580 during chromate reduction. Appl Surf Sci 202:150–159.

581 36. Goulhen F, Gloter A, Guyot F, Bruschi M. 2006. Cr(VI) detoxification by
582 *Desulfovibrio vulgaris* strain Hildenborough: Microbe-metal interactions
583 studies. Appl Microbiol Biotechnol 71:892–897.

584 37. Daulton TL, Little BJ, Lowe K, Jones-Meehan J. 2002. Electron energy loss
585 spectroscopy techniques for the study of microbial chromium(VI) reduction. J
586 Microbiol Methods 50:39–54.

587 38. Chardin B, Dolla A, Chaspoul F, Fardeau M, Gallice P, Bruschi M. 2003.
588 Bioremediation of chromate: Thermodynamic analysis of the effects of Cr(VI)
589 on sulfate-reducing bacteria. Appl Microbiol Biotechnol 60:352–360.

590 39. Stein LY, Yoon S, Semrau JD, DiSpirito AA, Crombie A, Murrell JC,
591 Vuilleumier S, Kalyuzhnaya MG, Op den Camp HJM, Bringel F, Bruce D,
592 Cheng JF, Copeland A, Goodwin L, Han S, Hauser L, Jetten MSM, Lajus A,
593 Land ML, Lapidus A, Lucas S, Medigue C, Pitluck S, Woyke T, Zeytun A, Klotz
594 MG. 2010. Genome sequence of the obligate methanotroph *Methylosinus*
595 *trichosporium* strain OB3b. J Bacteriol 192:6497–6498.

596 40. Ackerley DF, Gonzalez CF, Park CH, Blake R, Keyhan M, Matin A. 2004.

597 Chromate-reducing properties of soluble flavoproteins from *Pseudomonas*
598 *putida* and *Escherichia coli*. Appl Environ Microbiol 70:873–882.

599 41. Puzon GJ, Petersen JN, Roberts AG, Kramer DM, Xun L. 2002. A bacterial
600 flavin reductase system reduces chromate to a soluble chromium(III)-NAD^+
601 complex. Biochem Biophys Res Commun 294:76–81.

602 42. Barquera B, Hellwig P, Zhou W, Morgan JE, Häse CC, Gosink KK, Nilges M,
603 Bruesehoff PJ, Roth A, Lancaster CRD, Gennis RB. 2002. Purification and
604 characterization of the recombinant Na^+-translocating NADH:quinone
605 oxidoreductase from *Vibrio cholerae*. Biochemistry 41:3781–3789.

606 43. Daulton TL, Little BJ, Jones-Meehan J, Blom DA, Allard LF. 2007. Microbial
607 reduction of chromium from the hexavalent to divalent state. Geochim
608 Cosmochim Acta 71:556–565.

609 44. Villagrasa E, Ballesteros B, Obiol A, Millach L, Esteve I, Solé A. 2020. Multi-
610 approach analysis to assess the chromium(III) immobilization by
611 *Ochrobactrum anthropi* DE2010. Chemosphere 238:124663.

612 45. McLean JS, Beveridge TJ, Phipps D. 2000. Isolation and characterization of a
613 chromium-reducing bacterium from a chromated copper arsenate-
614 contaminated site. Environ Microbiol 2:611–619.

615 46. Hallberg R, Ferris FG. 2004. Biomineralization by Gallionella. Geomicrobiol J
616 21:325–330.

617 47. Edmunds WM, Darling WG, Purtschert R, Corcho Alvarado JA. 2014. Noble
618 gas, CFC and other geochemical evidence for the age and origin of the Bath
619 thermal waters, UK. Appl Geochemistry 40:155–163.

620 48. Challa S, Smith TJ. 2020. Isolation of a methane-oxidizing bacterium that
621 bioremediates hexavalent chromium from a formerly industrialized suburban
622 river. Lett Appl Microbiol lam.13330.

623 49. Lv P, Zhong L, Dong Q, Yang S, Shen W, Zhu Q, Lai C, Luo A-C, Tang Y,
624 Zhao H-P. 2018. The effect of electron competition on chromate reduction
625 using methane as electron donor. Environ Sci Pollut Res Int 25:6609–6618.

626 50. Lu YZ, Chen GJ, Bai YN, Fu L, Qin LP, Zeng RJ. 2018. Chromium isotope
627 fractionation during Cr(VI) reduction in a methane-based hollow-fiber
628 membrane biofilm reactor. Water Res 130:263–270.

629 51. Long M, Zhou C, Xia S, Guadiea A. 2017. Concomitant Cr(VI) reduction and
630 Cr(III) precipitation with nitrate in a methane/oxygen-based membrane biofilm
631 reactor. Chem Eng J 315:58–66.

632 52. Plaper A, Jenko-Brinovec Š, Premzl A, Kos J, Raspor P. 2002. Genotoxicity of
633 trivalent chromium in bacterial cells. Possible effects on DNA topology. Chem
634 Res Toxicol 15:943–949.

635 53. Fathima A, Rao JR. 2018. Is Cr(III) toxic to bacteria: toxicity studies using
636 *Bacillus subtilis* and *Escherichia coli* as model organism. Arch Microbiol
637 200:453–462.

638 54. Parker DL, Borer P, Bernier-Latmani R. 2011. The response of *Shewanella*
639 *oneidensis* MR-1 to Cr(III) toxicity differs from that to Cr(VI). Front Microbiol
640 2:1–14.

641 55. Pan X, Liu Z, Chen Z, Cheng Y, Pan D, Shao J, Lin Z, Guan X. 2014.
642 Investigation of Cr(VI) reduction and Cr(III) immobilization mechanism by

643 planktonic cells and biofilms of *Bacillus subtilis* ATCC-6633. Water Res 55:21–
644 29.

645 56. Cheng Y, Yan F, Huang F, Chu W, Pan D, Chen Z, Zheng J, Yu M, Lin Z, Wu
646 Z. 2010. Bioremediation of Cr(VI) and Immobilization as Cr(III) by
647 *Ochrobactrum anthropi*. Environ Sci Technol 44:6357–6363.

648 57. Stanley SH, Prior SD, Leak DJ, Dalton H. 1983. Copper stress underlies the
649 fundamental change in intracellular location of methane mono-oxygenase in
650 methane-oxidizing organisms: Studies in batch and continuous cultures.
651 Biotechnol Lett 5:487–492.

652 58. Gu W, Semrau JD. 2017. Copper and cerium-regulated gene expression in
653 *Methylosinus trichosporium* OB3b. Appl Microbiol Biotechnol 101:8499–8516.

654 59. Kao WC, Chen YR, Yi EC, Lee H, Tian Q, Wu KM, Tsai SF, Yu SSF, Chen YJ,
655 Aebersold R, Chan SI. 2004. Quantitative proteomic analysis of metabolic
656 regulation by copper ions in *Methylococcus capsulatus* (Bath). J Biol Chem
657 279:51554–51560.

658 60. Smith TJ, Murrell JC. 2011. Mutagenesis of soluble methane monooxygenase.
659 Methods Enzymol 495:135–147.

660 61. Smith TJ, Murrell JC. 2009. Methanotrophy/methane oxidation, p. vol. 3, pp.
661 293–298. *In* Schaechter, M (ed.), Encyclopedia of Microbiology, 3rd ed.
662 Elsevier B.V.

663 62. Smith TJ, Foster SJ. 2006. Autolysins during sporulation of *Bacillus subtilis*
664 168. FEMS Microbiol Lett 157:141–147.

665 63. Chen IMA, Chu K, Palaniappan K, Pillay M, Ratner A, Huang J, Huntemann M,
666 Varghese N, White JR, Seshadri R, Smirnova T, Kirton E, Jungbluth SP,
667 Woyke T, Eloe-Fadrosh EA, Ivanova NN, Kyrpides NC. 2019. IMG/M v.5.0: An
668 integrated data management and comparative analysis system for microbial
669 genomes and microbiomes. Nucleic Acids Res 47:D666–D677.

670

671 **FIGURE LEGENDS**

672

673 **FIG 1** Effect of *M. capsulatus* Bath cultures on Cr (VI) at various concentrations.
674 Experiments were biological triplicates. Experiments were biological triplicates.
675 Results are plotted as the ratio of supernatant chromium (VI) concentration (C) at
676 each time point to initial concentration (C_0) and are shown as mean ± SD. Parallel
677 triplicate controls without *M. capsulatus* Bath cells were performed at each initial
678 chromium (VI) concentration, which were constant to within 4 % of the initial
679 chromium (VI) concentration.

680

681 **FIG 2** Reduction and accumulation of chromium species by *M. capsulatus* Bath after
682 addition of Cr (VI) to 20 mg litre^{-1}. Values are the means from biological triplicates
683 and are shown as mean ± SD. Concentrations in each of the fractions were
684 normalised to the volume of the original culture.

685

686 **FIG 3** Speciation and distribution of chromium species analysed after fractionation of
687 cells into separate cell wall, cytoplasm and membrane fractions. Initial Cr (VI)
688 concentration was 20 mg litre^{-1}. Error bars show the standard deviation of three
689 biological replicates.

690

691 **FIG 4** Effect of adding 20 mg litre^{-1} of Cr (III) to *M. capsulatus* Bath cultures with and
692 without methane. The abiotic controls were culture medium plus methane in panel A
693 and culture medium without methane in panel B.

694

695

696 **FIG 5** EEL spectra of *M. capsulatus* Bath cells compared with chromium standards.
697 Inserts show the areas of the samples (circled) that were analysed by EELS. Initial Cr
698 (VI) concentration was 20 mg litre^{-1}.

699

700 **FIG 6** HADF-STEM and EDX of sectioned cells showing the distribution of chromium.
701 HAADF images of (A) cells without exposure to chromium; (B) cells exposed to 20 mg
702 litre^{-1} chromium (VI) for 144 h; (C) spatial distribution of chromium shown in the EDX
703 map of the sample shown in B. Green and yellow boxes on the micrographs in parts
704 A and B show the areas of the sample analysed in the EDX spectra of the samples
705 without (D) and with (E) exposure to chromium (VI).

706

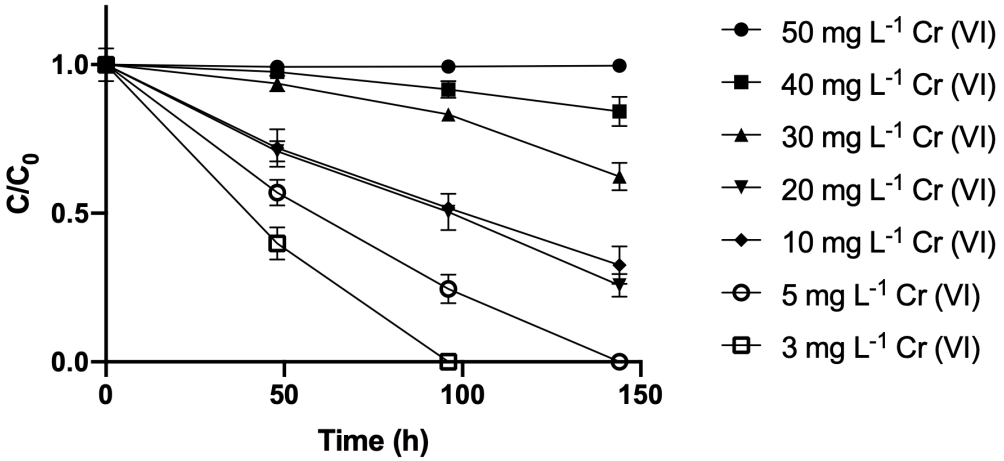
1.0
0.5
0.0
C/C0
0
50
100
150
Time (h)
50 mg L-1 Cr (VI)
40 mg L-1 Cr (VI)
30 mg L-1 Cr (VI)
20 mg L-1 Cr (VI)
10 mg L-1 Cr (VI)
5 mg L-1 Cr (VI)
3 mg L-1 Cr (VI)

707

708

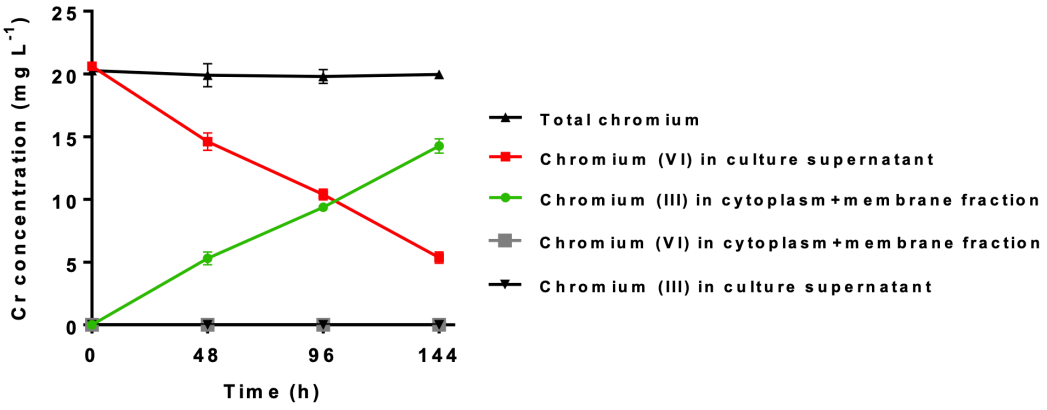
Cr concentration (mg L-1)
25
20
15
10
5
0
0
48
96
144
Time (h)
Total chromium
Chromium (VI) in culture supernatant
Chromium (III) in cytoplasm+membrane fraction
Chromium (VI) in cytoplasm+membrane fraction
Chromium (III) in culture supernatant

709

710

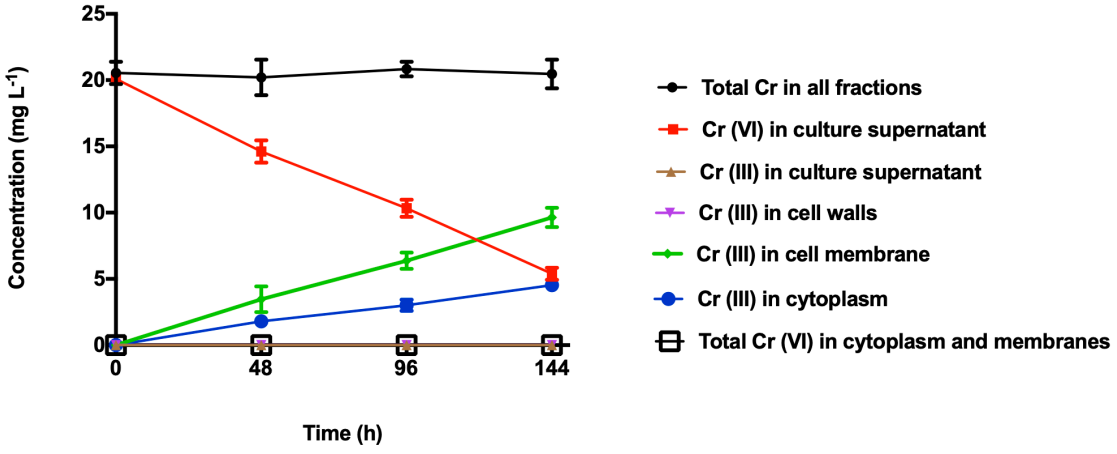
25
20
15
10
5
0
Concentration (mg L-1)
0
48
96
144
Time (h)
Total Cr in all fractions
Cr (VI) in culture supernatant
Cr (III) in culture supernatant
Cr (III) in cell walls
Cr (III) in cell membrane
Cr (III) in cytoplasm
Total Cr (VI) in cytoplasm and membranes

711

712

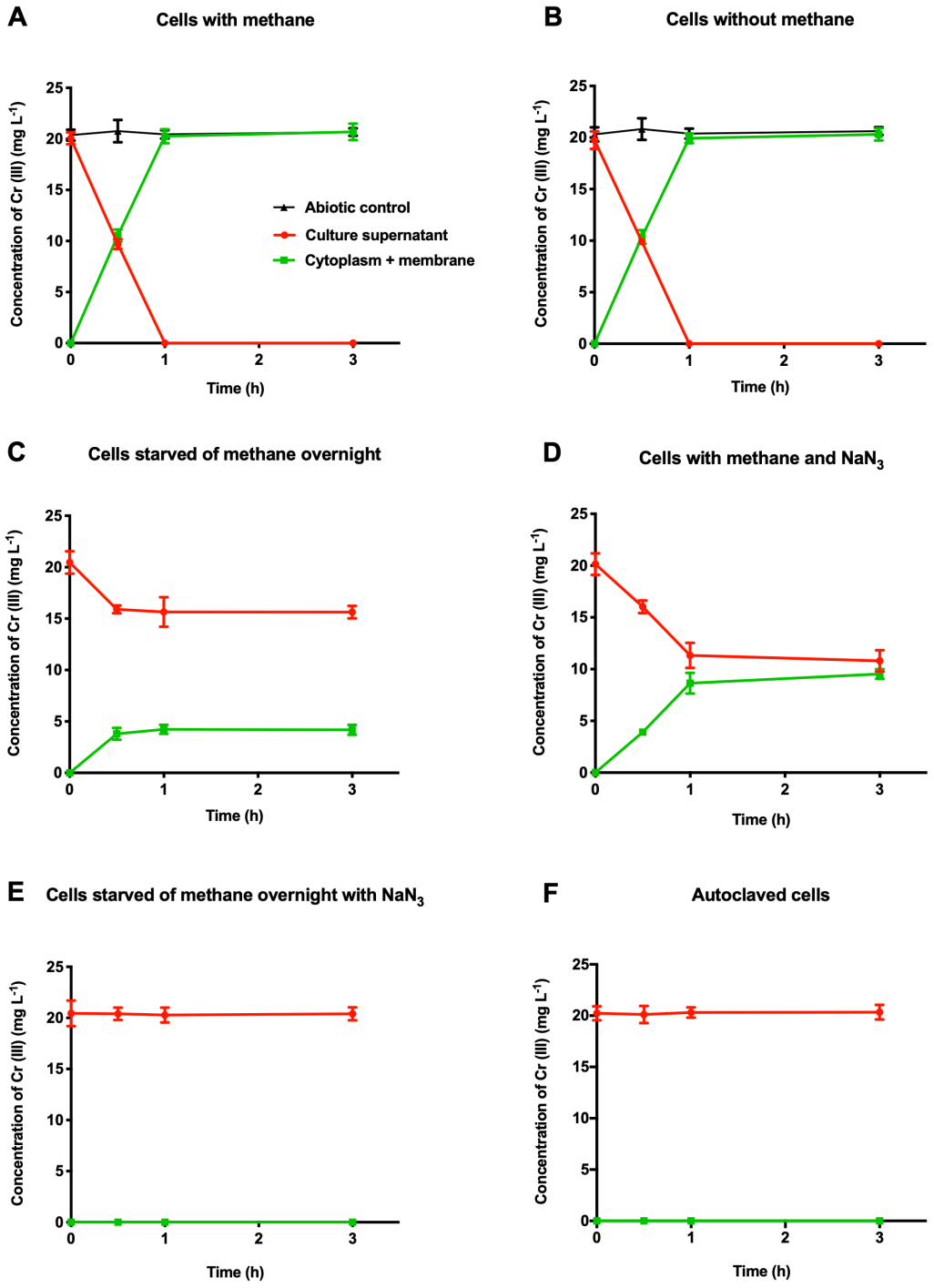
A
Cells with methane
B
Cells without methane
C
Cells starved of methane overnight
D
Cells with methane and NaN3
E
Cells starved of methane overnight with NaN3
F
Autoclaved cells
Concentration of Cr (III) (mg L-1)
Time (h)
Abiotic control
Culture supernatant
Cytoplasm + membrane

713

714

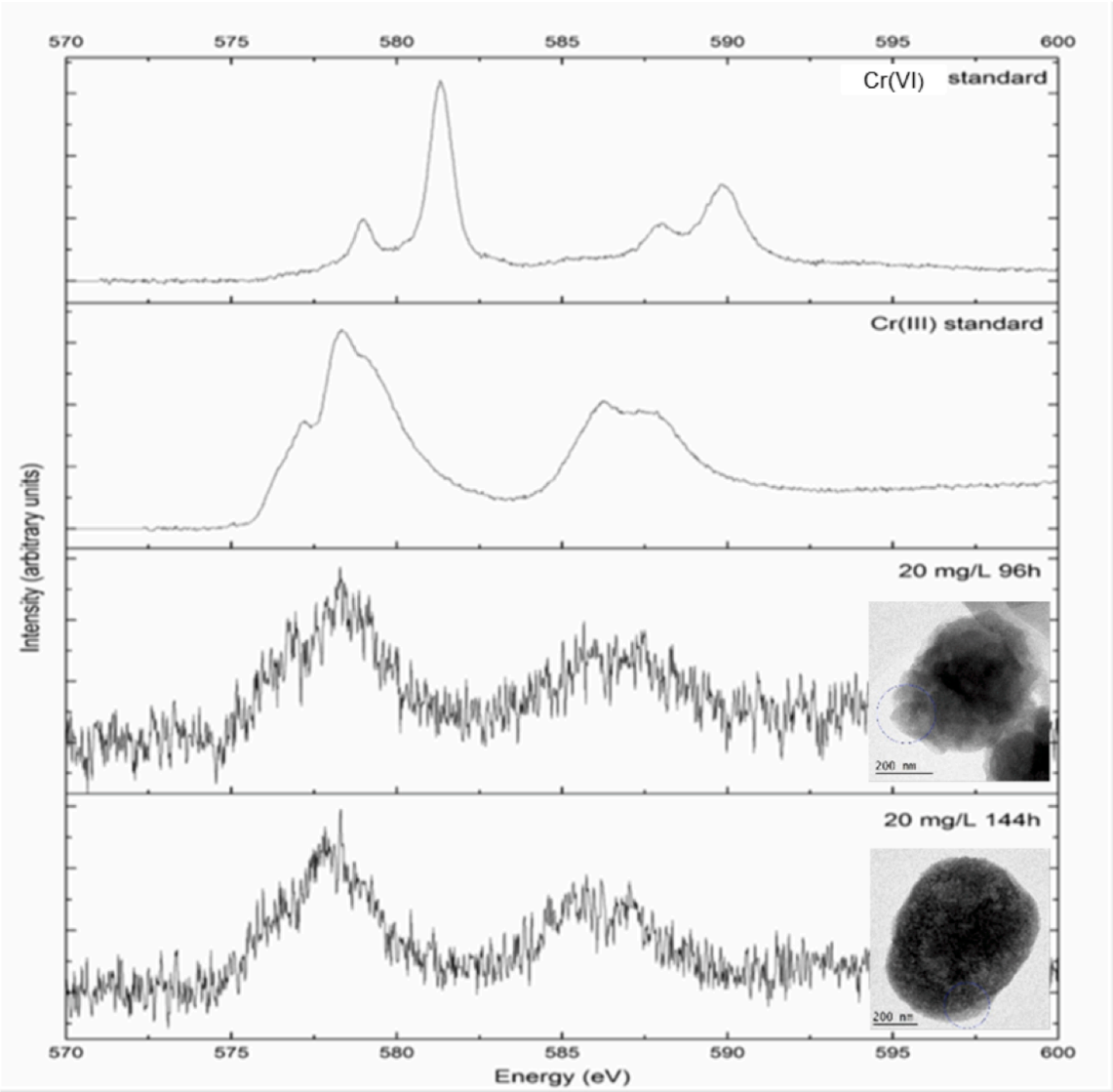
570
575
580
585
590
595
600
Cr(VI) standard
Cr(III) standard
20 mg/L 96h
200 nm
20 mg/L 144h
200 nm
Intensity (arbitrary units)
Energy (eV)

715

716

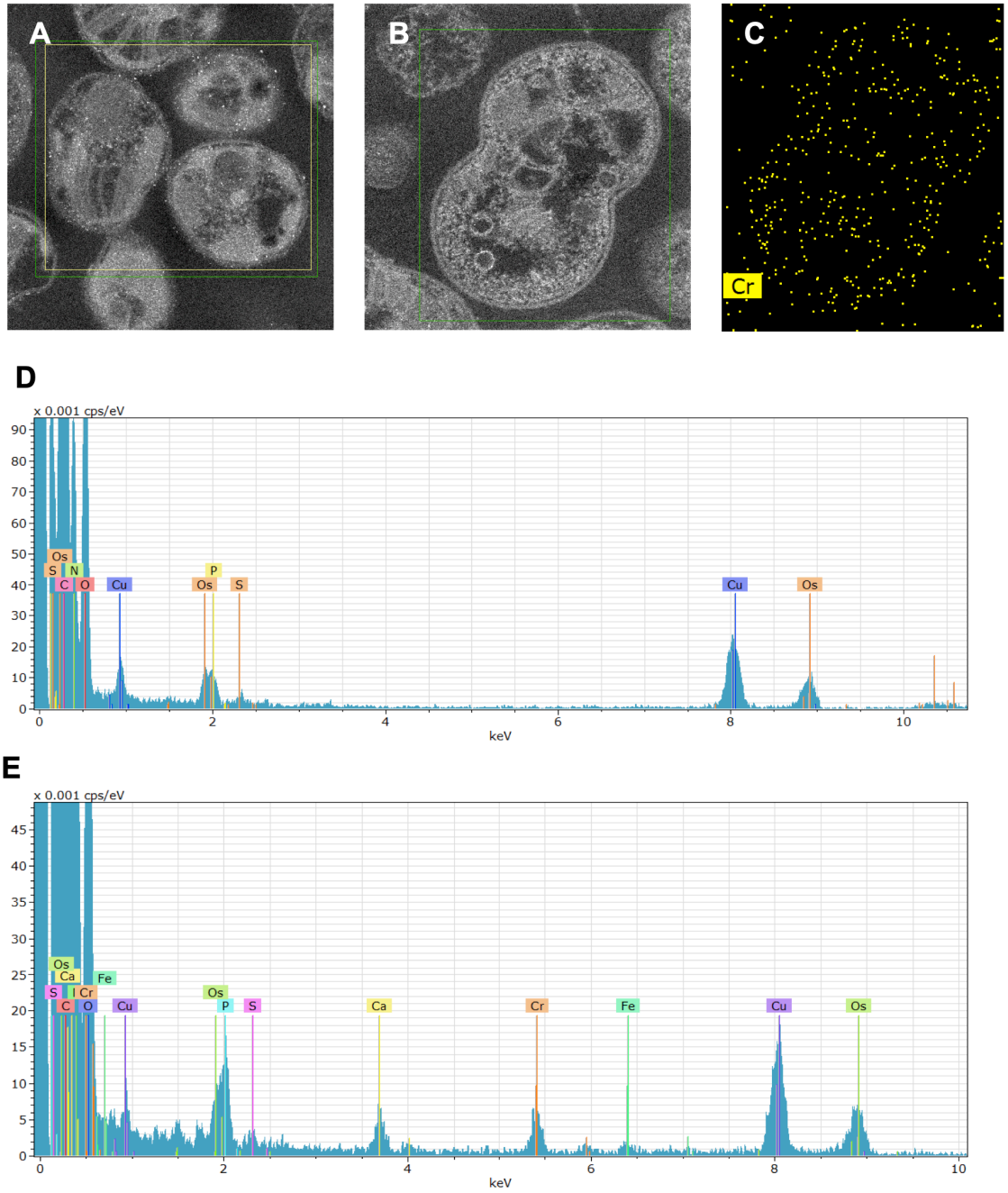
A
B
C
Cr
D
x 0.001 cps/eV
Os
S
N
C
O
Cu
P
Os
S
Cu
Os
keV
E
x 0.001 cps/eV
Os
Ca
Fe
S
Cr
C
O
Cu
Os
P
S
Ca
Cr
Fe
Cu
Os
keV

717

718

719 **Supplemental Material**

720

721 Detoxification, active uptake, and intracellular accumulation of chromium

722 species by a methane-oxidising bacterium

723

724 **Salaheldeen Enbaia [a], Abdurrahman Eswayah [a], Nicole Hondow [b], Philip H. E.**

725 **Gardiner [a] and Thomas J. Smith *,[a].**

726

727 [a] Biomolecular Sciences Research Centre, Sheffield Hallam University, Howard

728 Street, Sheffield S1 1WB, United Kingdom.

729 [b] School of Chemical and Process Engineering, University of Leeds, Leeds LS2 9JT,

730 United Kingdom.

731

732 * To whom correspondence should be addressed: Tel. +44 (0) 114 225 3042. Email:
733 t.j.smith@shu.ac.uk

734

735

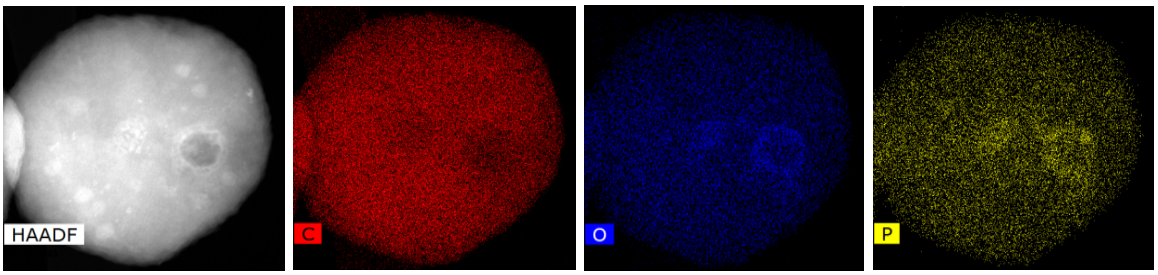

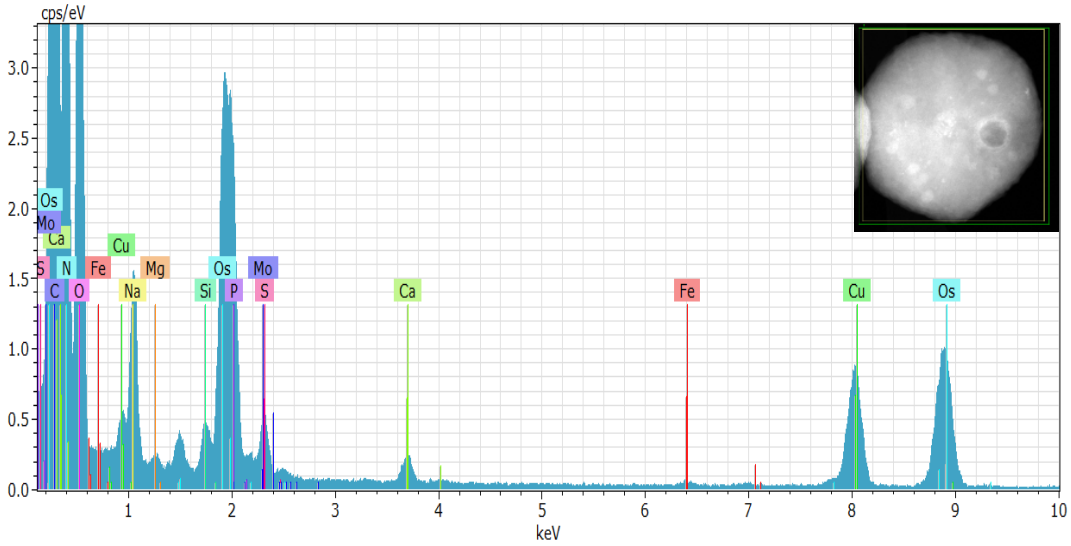

FIG S1 Electron micrographs with corresponding EDX spectra of whole *M. capsulatus* Bath cells, showing the distribution of carbon, oxygen and phosphorous after incubation of the culture in the presence of methane for 144 h at 45°C without added chromium. The EDX spectrum was generated from data collected from the area indicated by the box in the insert.

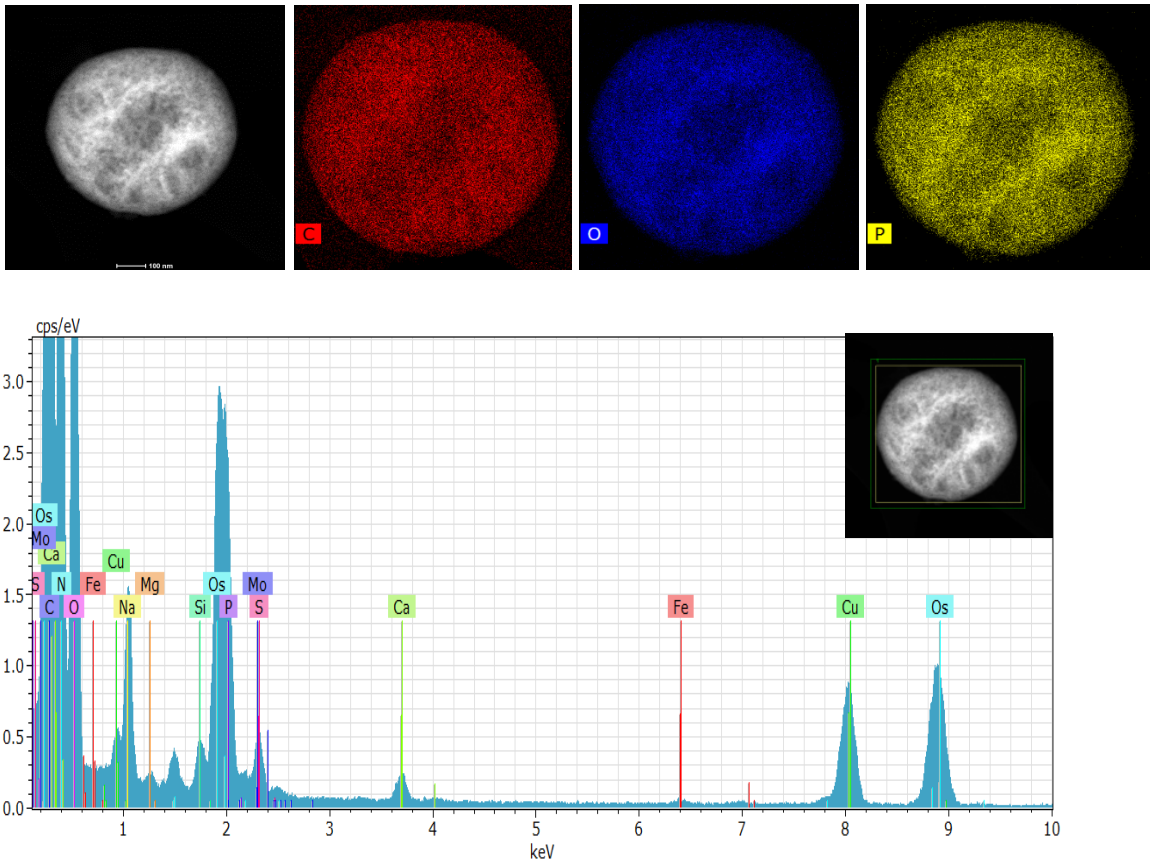

FIG S2 Electron micrographs showing the distribution of elements via EDX spectroscopy of whole *M. capsulatus* Bath cells, after incubation of the culture in the presence of methane for 144 h at 45°C without added chromium. The EDX spectrum was generated from data collected from the area indicated by the box in the insert. This figure shows a different area from the sample analysed in Fig. S1.

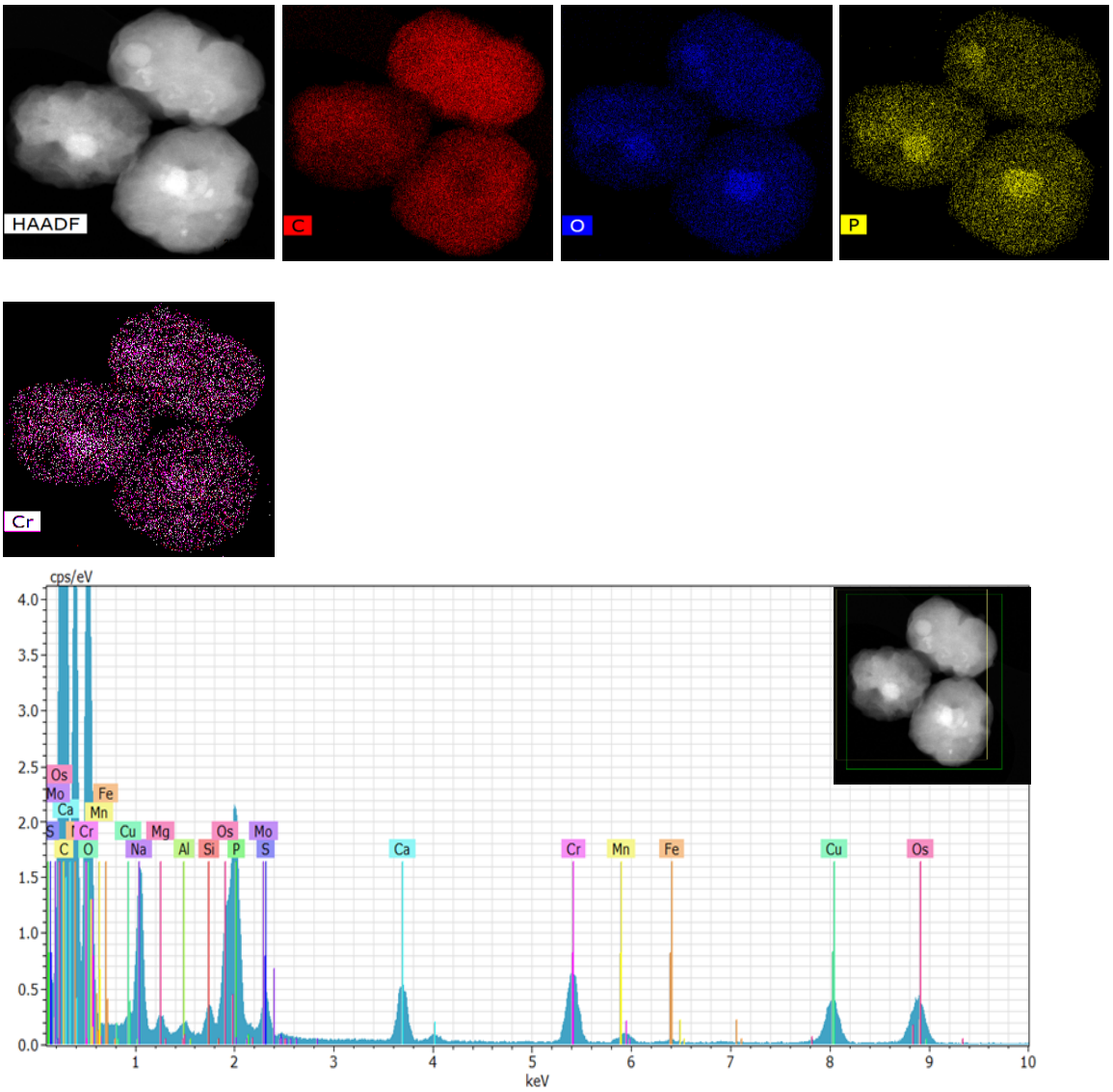

FIG S3 Electron micrographs with corresponding EDX spectra of whole *M. capsulatus* Bath cells, showing the distribution of carbon, oxygen and phosphorous after incubation of the culture in the presence of methane for 144 h at 45°C after addition of chromium (VI) to 20 mg L^{-1}. The EDX spectrum was generated from data collected from the area indicated by the box in the insert.

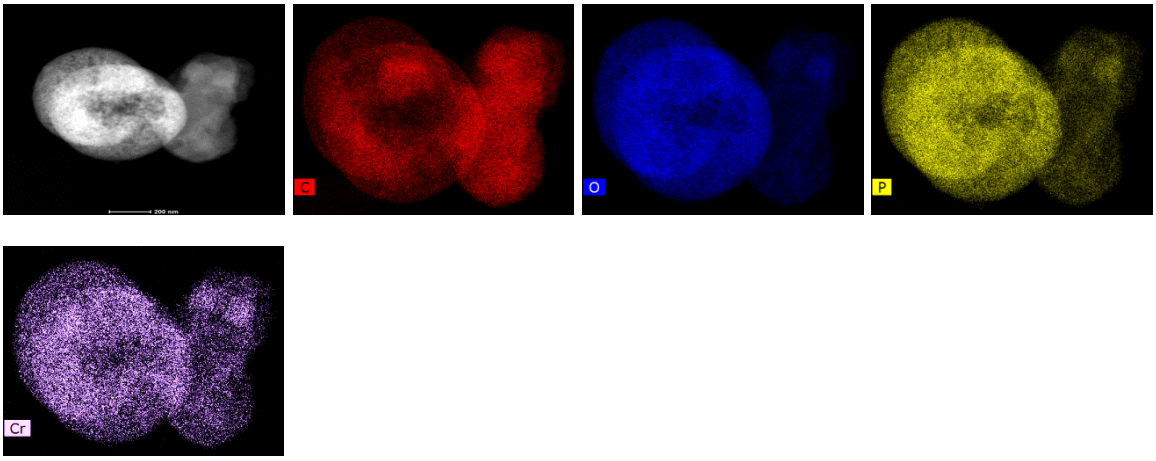

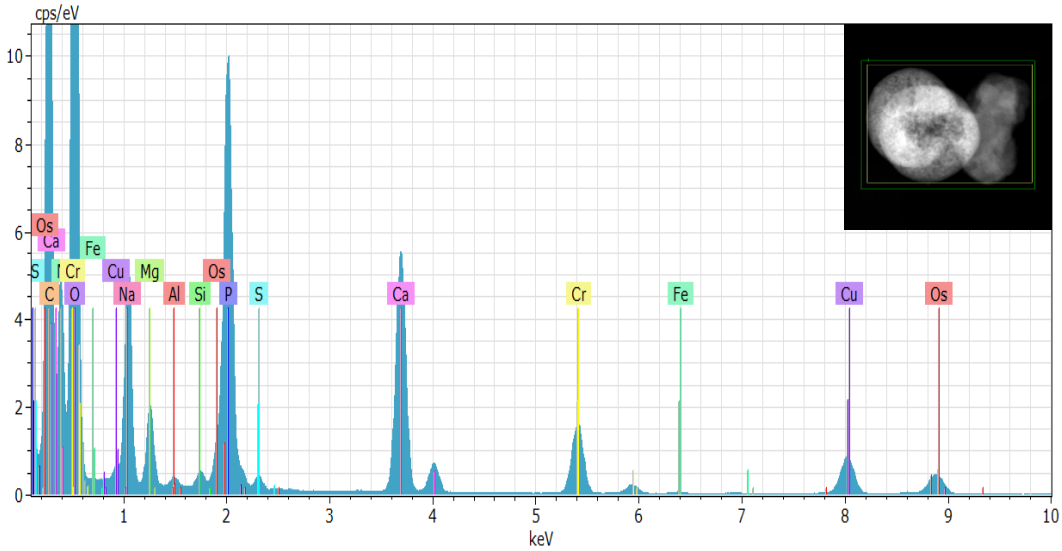

FIG S4 Electron micrographs showing the distribution of elements via EDX spectroscopy of whole *M. capsulatus* Bath cells, after incubation of the culture in the presence of methane for 144 h at 45°C after addition of chromium (VI) to 20 mg L^{-1}. The EDX spectrum was generated from data collected from the area indicated by the box in the insert. This figure shows a different area from the sample analysed in Fig. S3.

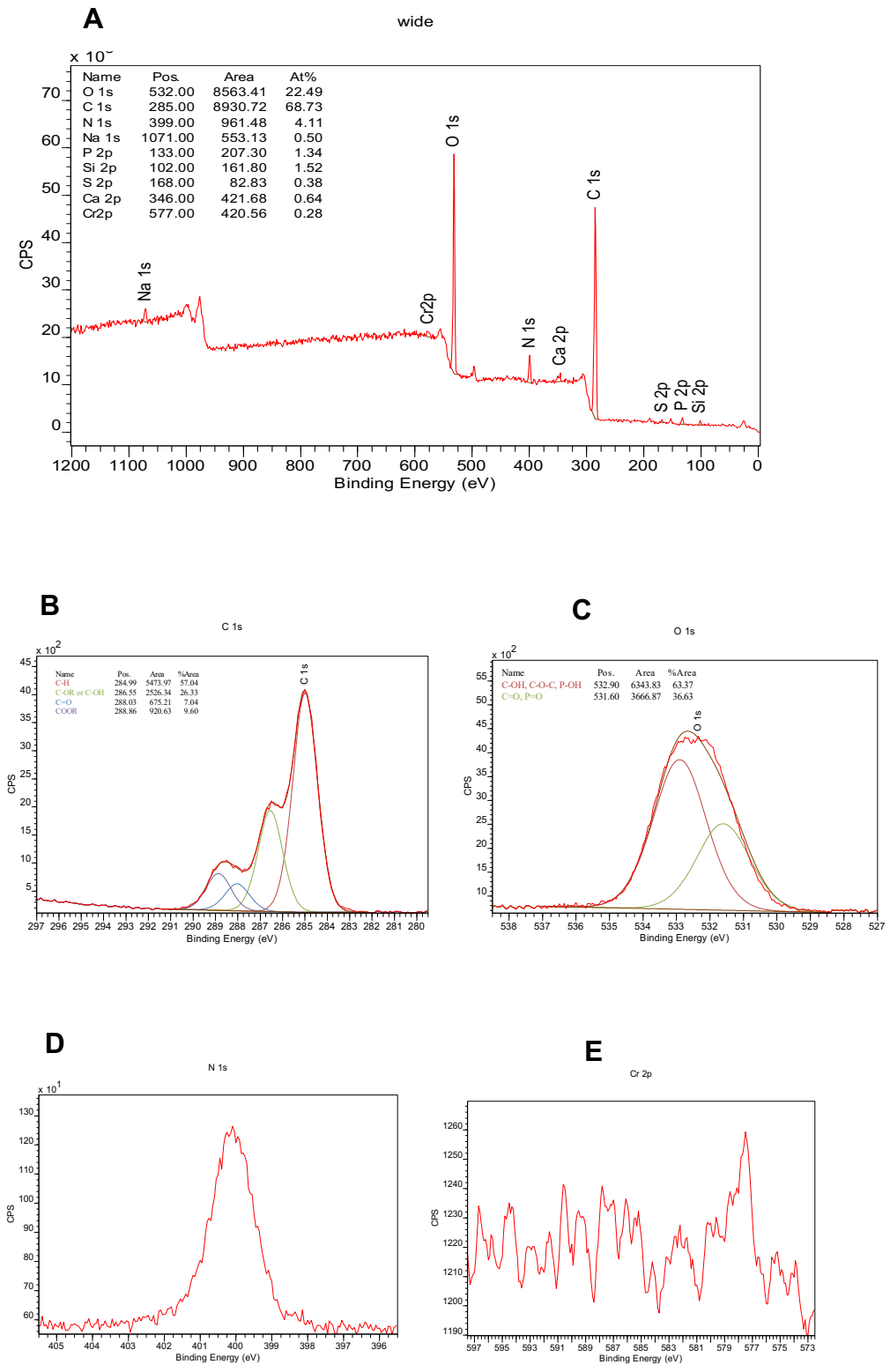

FIG S5 Wide scan X-ray photoelectron spectra of *M. capsulatus* Bath cells exposed to 20 mg L^{-1} of chromium (VI) for 144 h (A) and high resolution spectra for C 1s and O 1s are shown in B and C. The low resolution spectra for N 1s and Cr 2p are shown in D and E, respectively.

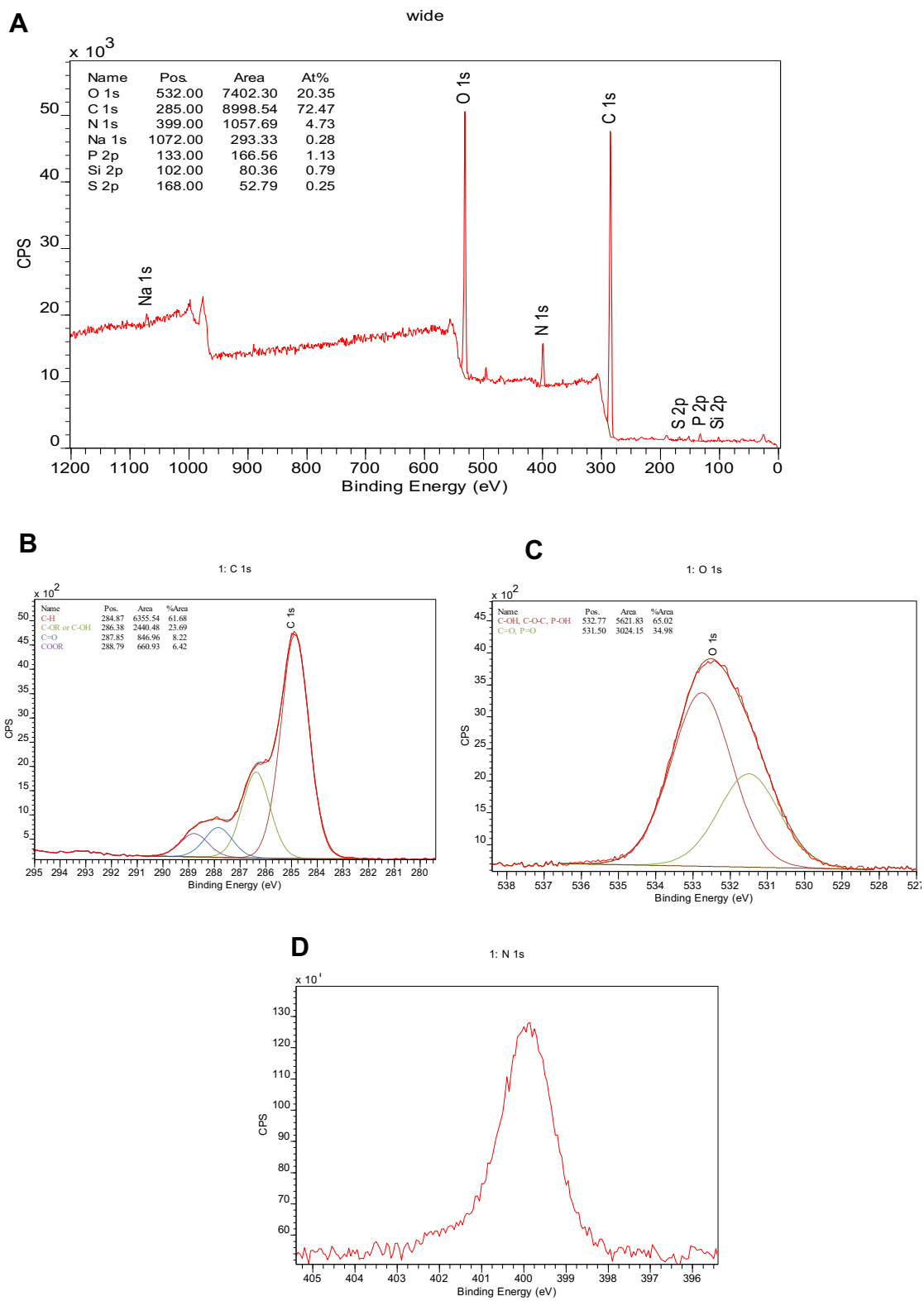

FIG S6 Wide scan X-ray photoelectron spectra of control sample to *M. capsulatus* Bath that was not exposed to chromium (A) and high resolution spectra for C 1s and O 1s are shown in B and C. The low resolution spectra for N 1s is shown in D.

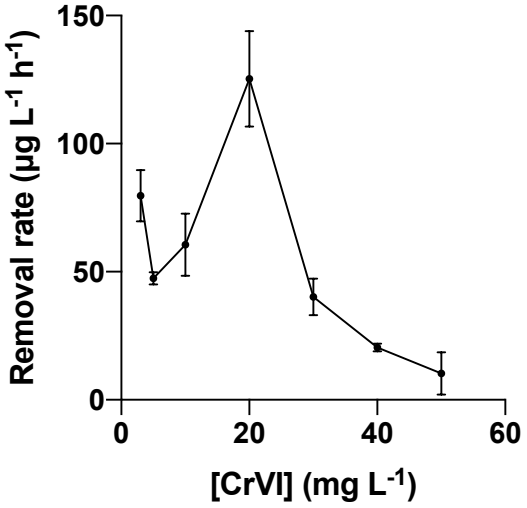

804

FIG S7 Rate of removal of chromium (VI) by cultures of *M. capsulatus* Bath calculated from the fall in chromium (VI) concentration during the first 24 h of incubation. Error bars show standard deviations of triplicate biological replicates. This graph was constructed using the same data used to construct Fig. 1 in the main text.

811 **TABLE S1.** Results of curve-appropriate C 1s spectra of *Mc. capsulatus* Bath of
812 (control sample compared with chromium-treated sample). (B. E. = binding energy).

Control sample			Chromium sample		
Name of group	B. E. (eV)	% Area	Name of group	B. E. (eV)	% Area
C - H	284.87	61.68	C - H	284.99	57.04
C- OR or C - OH	286.38	23.69	C- OR or C - OH	286.55	26.33
C = O	287.85	8.22	C = O	288.03	7.04
COOR	288.79	6.42	COOR	288.86	9.60

813

814 **TABLE S2.** Results of curve-appropriate O 1s spectra of *M. capsulatus* Bath of
815 (control sample compared with chromium-treated sample). (B. E. = binding energy).

Control sample			Chromium sample		
Name of group	B. E. (eV)	% Area	Name of group	B. E. (eV)	% Area
C - H, C - O - C, P - OH	532.77	65.02	C - H, C - O - C, P - OH	532.90	63.37
C = O, P = O	531.50	34.98	C = O, P = O	531.60	36.63

816

817

818

819 **TABLE S3.** Chromium (VI) reductase and permease homologues derived from
820 BLAST-P searches of the *M. capsulatus* Bath and *M. trichosporium* OB3b genomes.

821

Query sequence (accession number)	**Similar sequences** ($E < 10^{-5}$)	
	***M. capsulatus* Bath**	***M. trichosporium* OB3b**
Fre chromate reductase of *Escherichia coli* (M74448)	Soluble methane monooxygenase reductase component (locus tag MCA1200)	Soluble methane monooxygenase reductase component (locus tag Ga0263880_112528)
	Oxygenase, putative (MCA2508)	Ferredoxin-NADP reductase (Ga0263880_113028)
	Na(+)-translocating NADH-quinone reductase subunit F (MCA2384)	
Nitroreductase NfsA of *E. coli* (BAA35562)	Nitroreductase family protein (MCA1372)	Nitroreductase (Ga0263880_114180)
Old Yellow Enzyme chromate reductase of *Thermus scotoductus* (CAP16804)	NADH-dependent flavin oxidoreductase, Oye family (MCA0639)	2,4-dienoyl-CoA reductase-like NADH-dependent reductase (Old Yellow Enzyme family) (Ga0263880_11482)
ChrR chromate reductase of *Pseudomonas putida* (Q93T20)	None	NAD(P)H-dependent FMN reductase (Ga0263880_113996)
ChrA chromate efflux pump of *Pseudomonas aeruginosa* plasmid pUM505 (M29034)	None	None

822

823